

Autler-Townes splitting in two-color photoassociation of ${}^6\text{Li}$

U. Schlöder, T. Deuschle, C. Silber, and C. Zimmermann

Physikalisches Institut, Eberhard Karls Universität, Auf der Morgenstelle 14, 72076 Tübingen, Germany

(Received 16 April 2003; published 26 November 2003)

We report on high-resolution two-color photoassociation spectroscopy in the triplet system of magneto-optically trapped ${}^6\text{Li}$. Photoassociation is induced from the ground-state asymptote to the $v=59$ level of the excited $1^3\Sigma_g^+$ state. This level is coupled to the $v=9$ level of the triplet ground state $a^3\Sigma_u^+$ by the light field of a Raman laser. The absolute transition frequencies are measured with an iodine frequency standard and the binding energy of the ground state is determined to be 24.391 ± 0.020 GHz. Strong coupling of the bound molecular states has been observed as Autler-Townes splitting in the photoassociation signal for different detunings of the Raman laser. From the splitting we determine the spontaneous bound-bound decay rate to be $4.3 \times 10^5 \text{ s}^{-1}$ and estimate the molecule formation rate. The observed line shapes are in good agreement with the theoretical model.

DOI: 10.1103/PhysRevA.68.051403

PACS number(s): 32.80.Pj, 33.80.Ps, 34.20.Cf, 42.50.Hz

Coherent coupling schemes offer intriguing novel possibilities for the production of cold molecules. In such schemes, the continuum state of a free atom pair is coupled to a rovibrational level of the molecular ground state. Magnetic coupling in the vicinity of a Feshbach resonance has led to the observation of atom-molecule coherence in a ${}^{85}\text{Rb}$ Bose-Einstein condensate (BEC) [1] and to the selective production of weakly bound Cs_2 dimers [2]. Optical coupling in stimulated Raman transitions has allowed for the creation of ${}^{87}\text{Rb}$ molecules in a BEC [3] and of Cs_2 molecules from a magneto-optically trapped atomic cloud [4]. In contrast to single-color photoassociation experiments, where cold ground-state molecules are produced incoherently by spontaneous decay of the optically excited dimer [5–7], these transition schemes have coherent character. Thereby, ground-state molecules are produced in a specific rovibrational level. In addition, the molecule formation rate can be strongly enhanced, as it is not limited by the small branching ratio between the bound-bound and the bound-free transitions. This is especially important for the formation of dimers with small intrinsic molecule formation rates, as in case of the absence of any favorable peculiarities in their potentials [5,7]. While magnetic coupling schemes require a Feshbach resonance at sufficiently low magnetic fields and allow only for the production of cold molecules in weakly bound states, optical coupling schemes are more universal. Moreover, in extended multicolor versions, they are proposed for the production of molecules which are not only translationally, but also vibrationally cold [8].

Among the cold homonuclear dimers, ${}^6\text{Li}_2$ molecules in the triplet state are particularly interesting. Combining two ${}^6\text{Li}$ atoms to a ${}^6\text{Li}_2$ molecule corresponds to transferring a fermionic system into a bosonic system. Such transition schemes are a prerequisite for studying the effects of different quantum statistics on the reaction dynamics, the so-called superchemistry [9]. If, in addition, the molecule is prepared in the triplet state, it has a magnetic dipole moment. Storing these cold molecules in a magnetic trap should be possible, as demonstrated for cesium triplet dimers in a magnetic quadrupole trap recently [10].

In this paper we report on two-color photoassociation in the triplet system of ${}^6\text{Li}_2$. We use a Raman-type coupling scheme as shown in Fig. 1. Photoassociation is induced from the hyperfine ground-state asymptote $f=1/2+f=3/2$ into the excited triplet $1^3\Sigma_g^+$ state by the photoassociation laser with frequency ν_{PA} . From the excited rovibrational level $v=59$, $N=1$, the specific hyperfine state $|1111\rangle$ ($|NSIG\rangle$ notation, see, e.g., Ref. [11]) is selected. The excited level lies at a laser detuning of -1787 GHz relative to the $D1$ -line, corresponding to a Condon point of about $34a_0$. The natural linewidth is approximately twice the atomic value Γ and amounts to $2\pi \times 11.7$ MHz [12]. The Raman laser of the frequency ν_{R} couples the excited state to the hyperfine state $|0111\rangle$ of the $v=9$, $N=0$ level of the triplet ground state $a^3\Sigma_u^+$. The ground-state level has a binding energy of approximately -24 GHz and an outer turning point of $27a_0$. The binding energies and the hyperfine structure involved in this scheme have been determined in photoassociation experiments of R. Hulet and co-workers [11,13]. In our experiments we focus on an absolute frequency measurement of the bound-free and the bound-bound transition and therefrom

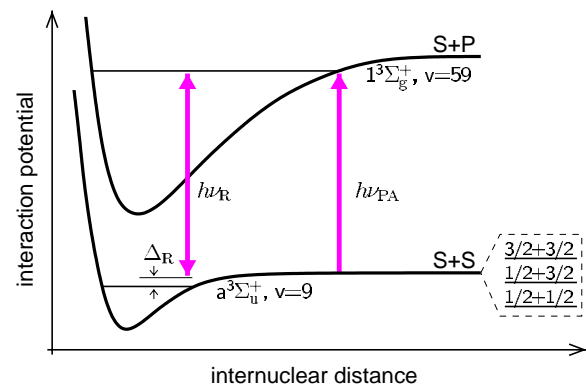


FIG. 1. Coupling scheme for the stimulated Raman photoassociation in the triplet system of the ${}^6\text{Li}_2$ molecule. Photoassociation is induced from the ground-state asymptote $1/2+3/2$ into the hyperfine state $|1111\rangle$ of the excited level $v=59$. The Raman laser couples this excited level to the hyperfine state $|0111\rangle$ of the ground-state vibrational level $v=9$.

we deduce the binding energy of the ground state. Furthermore, we study the influence of the detuning of the fixed Raman laser on the photoassociation signal. Autler-Townes splitting in the two-color photoassociation signal is observed, which arises from the strong coupling of the bound molecular states. We discuss the line shape in the light of the theory of Bohn and Julienne [14]. From the amount of the splitting we deduce the spontaneous decay rate and estimate the molecule formation rate. These results on the Autler-Townes splitting are complementary to recent two-color photoassociation experiments with cesium [4].

For the magneto-optical trap we use the two-species apparatus as described in Ref. [15], but operate it with ^6Li only. We apply a detuning of -5Γ for the cooling transition and of -2Γ for the repumping transition. The temperature of the atomic ensemble can be estimated to be 0.5 mK [16]. The particle number is monitored by absorption from a weak probe beam. For the photoassociation light we use a grating-stabilized diode laser with an output power of 12 mW. The light of the Raman beam is derived from a dye laser with 500 mW output power. The two laser beams are superimposed with parallel polarization and adjustable relative laser powers. The $1/e^2$ diameters of the laser beams at the position of the atomic cloud amount to 550 μm , corresponding to peak intensities of up to $I_R = 40 \text{ W/cm}^2$ for the Raman laser and of up to $I_{PA} = 7 \text{ W/cm}^2$ for the photoassociation laser. The stabilization and tuning of the diode laser is achieved by means of a stabilization chain. The diode is locked to a Fabry-Perot etalon with 300 MHz free spectral range. This etalon is stabilized relative to a second diode laser, which is again stabilized to a reference diode laser by a heterodyne technique. This reference laser is locked to an atomic lithium resonance by radio-frequency sideband spectroscopy in a lithium cell. Absolute frequency calibration is achieved by a Doppler-free iodine fluorescence spectroscopy with an accuracy of 10 MHz [17]. The scan rate is chosen to be 0.5–1 MHz/s for the absolute frequency measurements and 0.36 MHz/s for the Autler-Townes measurements. This is slow as compared to the loading time of the trap of 15 s. Thereby, a resolution of a few MHz is achieved.

For the absolute frequency measurement of the photoassociation and the Raman transition we proceed in the following manner. First, we record the single-color photoassociation spectrum and the iodine spectrum in the relevant frequency range simultaneously. For this special case we use the dye laser to induce photoassociation because of its larger tuning range. In order to keep the influence of the light shift [18] small, we reduce the laser intensity to 3 W/cm^2 . For the transition from the hyperfine ground-state asymptote $f = 1/2 + f = 3/2$ into the specific excited hyperfine state we determine the frequency to be $445\,002.881 \pm 0.015 \text{ GHz}$. A redshift of 10 MHz due to the thermal energy of the atoms has been included in this analysis. Then, the photoassociation laser is held fixed on this transition, which leads to a decrease in the steady-state particle number of the trapped atoms to 75%. The Raman laser is scanned with an intensity of 10 W/cm^2 . An increase in the particle number reveals the resonance frequency of the Raman laser with the bound-bound transition, which lies at $445\,027.272 \pm 0.013 \text{ GHz}$

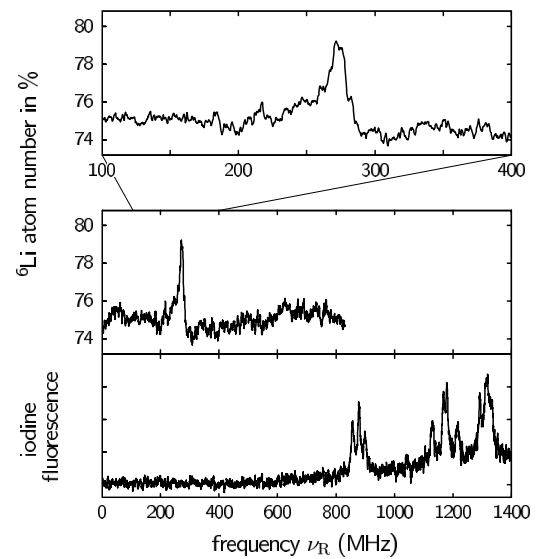


FIG. 2. Two-color photoassociation spectrum and iodine reference spectrum in the case of a fixed photoassociation laser and a scanned Raman laser. The offset to the axis of the Raman laser frequency ν_R is 445 027 GHz.

(Fig. 2). At our relatively high Raman laser intensities, this reduction of decrease originates from the strong coupling of the bound molecular states by the Raman laser (see below), as a consequence, the photoassociation laser is no longer resonant with the free-bound transition and particle losses due to photoassociation are suppressed. The binding energy of the bound ground-state level $v = 9$ in the absence of hyperfine structure is equivalent to the difference between the measured transition frequencies, because the initial and final levels are shifted due to the hyperfine structure by the same amount. We obtain a value of $24.391 \pm 0.020 \text{ GHz}$. The uncertainty is mainly due to a possible systematic error in the iodine reference spectrum and moreover due to the error in the determination of the line position. Our result is in agreement with the value of $24.43 \pm 0.02 \text{ GHz}$ obtained from a direct measurement of the frequency difference [11].

The line shape of the two-photon signal shows strong asymmetries with a shallow slope at the low-frequency side and a steep slope at the high-frequency side. We determine the linewidth (full width at half maximum) to be 15 MHz. Therewith, the linewidth is smaller than the convolution of the natural linewidth of 11.7 MHz and the thermal broadening of about 10 MHz. The line shape is that of a typical Fano profile [19,20], which has been analyzed experimentally in Ref. [21].

For the Autler-Townes measurements, we first tune the Raman laser in resonance with the bound-bound transition for calibration. Then, a fixed detuning Δ_R is added and the photoassociation laser is scanned. Two-color photoassociation spectra for three different detunings Δ_R of the Raman laser are shown in Fig. 3. The spectrum in the middle has been taken in the presence of a resonant Raman laser ($\Delta_R = 0 \text{ MHz}$). For the outer spectra, the Raman laser was detuned by the same amount of 30 MHz to the red and to the blue, respectively. For these spectra, the laser intensities

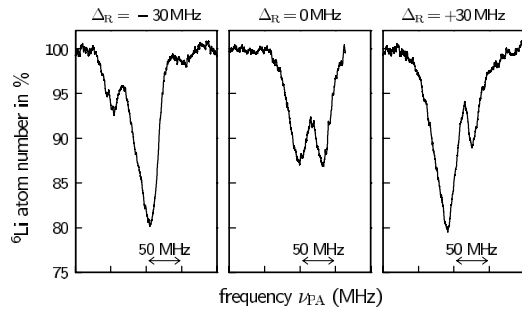


FIG. 3. Autler-Townes splitting for three different detunings Δ_R of the Raman laser. The axis of the photoassociation laser frequency ν_{PA} shows relative frequency calibration.

were chosen to be 30 W/cm^2 for the Raman laser and 3 W/cm^2 for the photoassociation laser. All three resonances show a doublet structure with a splitting of several 10 MHz. In the case of the resonant Raman laser, the resonance is split into two peaks with equal depth. For a detuned Raman laser, the splitting is asymmetric with a larger peak on the high-frequency side for red detuning and with a larger peak on the low-frequency side for blue detuning. To determine the splitting we fit two Lorentzian functions to the data. For the resonant Raman laser the spacing between the maxima of the resonances amounts to 34.6 MHz. For the detuned Raman laser the spacing is 50.1 MHz and 40.4 MHz, respectively.

The origin of the splitting can be explained in the dressed-state picture [20]. Here, the two bound molecular states are dressed with the light field of the Raman laser, forming a ladder of doublets that are separated by the generalized Rabi frequency $\Omega_{\text{gen}}/2\pi$. Its value depends on the detuning Δ_R of the Raman laser and of the Rabi frequency Ω (see below) according to $\Omega_{\text{gen}}/2\pi = \sqrt{\Delta_R^2 + (\Omega/2\pi)^2}$. By probing the system from a third level with a weak laser beam, this splitting appears as an Autler-Townes doublet [22]. In the case considered here, this third level corresponds to the continuum state.

A more sophisticated model, also including line shapes, is given by Bohn and Julienne [14]. This description is based on scattering theory and yields a general analytic expression for the two-color photoassociation scattering probability $|S|^2$. For a thermal ensemble, the corresponding rate coefficient K is obtained by thermal averaging. The results of a simulation for the corresponding parameters of our experiment are shown in Fig. 4. In this theory, the origin of the splitting is explained by two maxima of the scattering probability $|S|^2$ as a function of the photoassociation laser frequency ν_{PA} . The magnitude of the splitting is independent of the scattering energy E and corresponds to the generalized Rabi frequency Ω_{gen} . By thermal averaging over the scattering energies, the different resonance widths in the scattering probability $|S|^2$ translate into different heights of the doublet peaks of the rate coefficient K . However, thermal averaging does not change the amount of the splitting substantially, which we have checked for various parameters. The thermal averaged resonances are asymmetric. The high-frequency sides are always steeper. This is due to the convolution of the small intrinsic linewidth of the transition with the Boltzmann

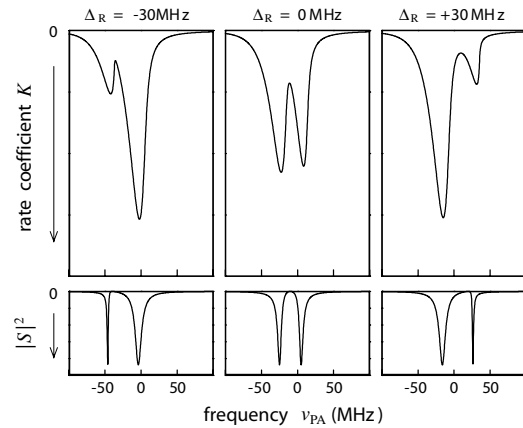


FIG. 4. Scattering probability $|S|^2$ for a scattering energy of $E/h = 10 \text{ MHz}$ and rate coefficient K for a temperature of 0.5 mK for three different detunings Δ_R of the Raman laser. For the Rabi frequency $\Omega = 2\pi \times 30 \text{ MHz}$ and for the natural linewidth $\gamma = 12 \text{ MHz}$ were assumed. The frequency axis is relative to the transition frequency for vanishing energy. To compare the calculation with the experimental data, the ordinate is plotted upside down.

distribution of the scattering energies E . Thereby, contributions from low energies, corresponding to higher frequencies, are favored.

The measured trap loss (Fig. 3) is proportional to the calculated photoassociation rate coefficient K (Fig. 4), if a linear response of the steady-state particle number to the rate coefficient K is assumed. For low photoassociation laser intensities this approximation is justified. The agreement concerning the splitting and the relative heights of the peaks between experiment and theory is quite good. Moreover, the asymmetry due to the thermal averaging is visible in the experimental spectra, particularly for the spectrum with $\Delta_R = -30 \text{ MHz}$.

For the experimental determination of the Rabi frequency Ω , we use the data taken for a resonant Raman laser. In this case the generalized Rabi frequency Ω_{gen} is identical to the Rabi frequency Ω and independent of uncertainties in the detuning of the Raman laser. Therefore, the measured splitting of 34.6 MHz can be identified with the Rabi frequency $\Omega/2\pi$. By using the relation for the Rabi frequency $\Omega = \sqrt{3c^2 I_R \Gamma_{bb}/4\pi h \nu_R^3}$, we determine the transition rate Γ_{bb} between the bound states to be $4.3 \times 10^5 \text{ s}^{-1}$. This coincides well with a value of $6.16 \times 10^5 \text{ s}^{-1}$ [8], derived theoretically from a simplified two-level system.

The experimental data allow an estimation of the molecular formation rate per atom and per second. For the resonant Raman laser, each doublet peak consists of contributions from the molecular ground state and from the excited state to equal parts. Thereby, the molecule formation rate should be given by half the single-color photoassociation rate. The photoassociation rate itself can be estimated from the 87% reduction of the steady-state number of ^6Li atoms in presence of the photoassociation laser (see Fig. 3). Assuming constant density and using the measured value for the loading time of the trap, we use the formula given in Ref. [23]. We receive a value for the photoassociation rate in the range

of 0.01 s^{-1} per atom, leading to a molecule formation rate of the same order of magnitude. This is an enhancement by a factor of 100 compared to the molecule formation rate due to single-color photoassociation, which can be estimated to be $8.4 \times 10^{-5} \text{ s}^{-1}$ by multiplying the photoassociation rate with the branching ratio between the bound-bound and the free-bound transitions [8]. For typical particle numbers of the order of 10^8 atoms [15], the absolute molecule formation rate amounts to 10^6 molecules/s. However, in order to estimate the number of formed molecules, loss processes, such as spontaneous Raman scattering, have to be taken into account.

In conclusion, we have performed high-resolution two-color photoassociation spectroscopy in the triplet system of the $^6\text{Li}_2$ molecule. The binding energy of the last bound

level of the ground state has been determined in an absolute frequency measurement. We have observed the Autler-Townes splitting in the two-color photoassociation signal and therefrom deduced the bound-bound transition rate and the molecule formation rate. This rate is sufficiently high to encourage future experiments in this transition scheme. These are the accumulation of the cold triplet dimers in a magnetic trap and the production of vibrationally cold ground-state molecules via multicolor photoassociation schemes. For the degenerate regime, even pulsed schemes such as STIRAP [24] are discussed.

We would like to thank H. Schnatz and B. Bodermann from the PTB Braunschweig and E. Tiemann for valuable help with the iodine spectroscopy. This work has been partially funded by the Deutsche Forschungsgemeinschaft.

-
- [1] E.A. Donley, N.R. Claussen, S.T. Thompson, and C.E. Wieman, *Nature (London)* **417**, 529 (2002).
- [2] C. Chin, A.J. Kerman, V. Vuletić, and S. Chu, *Phys. Rev. Lett.* **90**, 033201 (2003).
- [3] R. Wynar, R.S. Freeland, D.J. Han, C. Ryu, and D.J. Heinzen, *Science* **287**, 1016 (2000).
- [4] B. Laburthe Tolra, C. Drag, and P. Pillet, *Phys. Rev. A* **64**, 061401(R) (2001).
- [5] A. Fioretti, D. Comparat, A. Crubellier, O. Dulieu, F. Masnou-Seeuws, and P. Pillet, *Phys. Rev. Lett.* **80**, 4402 (1998).
- [6] A.N. Nikolov, E.E. Eyler, X.T. Wang, J. Li, H. Wang, W.C. Stwalley, and P.L. Gould, *Phys. Rev. Lett.* **82**, 703 (1999).
- [7] C. Gabbanini, A. Fioretti, A. Lucchesini, S. Gozzini, and M. Mazzoni, *Phys. Rev. Lett.* **84**, 2814 (2000).
- [8] R. Côté and A. Dalgarno, *J. Mol. Spectrosc.* **195**, 236 (1999).
- [9] D.J. Heinzen, R. Wynar, P.D. Drummond, and K.V. Kheruntsyan, *Phys. Rev. Lett.* **84**, 5029 (2000).
- [10] N. Vanhaecke, W. de Souza Melo, B. Laburthe Tolra, D. Comparat, and P. Pillet, *Phys. Rev. Lett.* **89**, 063001 (2002).
- [11] E.R.I. Abraham, W.I. McAlexander, J.M. Gerton, R.G. Hulet, R. Côté, and A. Dalgarno, *Phys. Rev. A* **55**, R3299 (1997).
- [12] R. Côté and A. Dalgarno, *Phys. Rev. A* **58**, 498 (1998).
- [13] E.R.I. Abraham, W.I. McAlexander, H.T.C. Stoof, and R.G. Hulet, *Phys. Rev. A* **53**, 3092 (1996).
- [14] J.L. Bohn and P.S. Julienne, *Phys. Rev. A* **54**, R4637 (1996).
- [15] U. Schlöder, C. Silber, and C. Zimmermann, *Appl. Phys. B* **73**, 801 (2001).
- [16] U. Schünemann, H. Engler, M. Zielonkowski, M. Weidemüller, and R. Grimm, *Opt. Commun.* **158**, 263 (1998).
- [17] C. Silber, T. Deuschle, U. Schlöder, S. Günther, and C. Zimmermann, in *Interactions in Ultracold Gases: From Atoms to Molecules*, edited by M. Weidemüller and C. Zimmermann (Wiley-VCH, Weinheim, 2003).
- [18] J.L. Bohn and P.S. Julienne, *Phys. Rev. A* **60**, 414 (1999).
- [19] U. Fano, *Phys. Rev.* **124**, 1866 (1961).
- [20] C. Cohen-Tannoudji, J. Dupont-Roc, and G. Grynberg, *Atom-Photon Interactions* (Wiley, New York, 1998).
- [21] C. Lisdat, N. Vanhaecke, D. Comparat, and P. Pillet, *Eur. Phys. J. D* **21**, 299 (2002).
- [22] S.H. Autler and C.H. Townes, *Phys. Rev.* **100**, 703 (1955).
- [23] U. Schlöder, C. Silber, T. Deuschle, and C. Zimmermann, *Phys. Rev. A* **66**, 061403(R) (2002).
- [24] A. Vardi, D. Abrashkevich, E. Frishman, and M. Shapiro, *J. Chem. Phys.* **107**, 6166 (1997).